Numerical Analysis for un-baffled Mixing Tank Agitated by Two Types of Impellers

Ammar Ashour Akesh
College of Engineering, University of Basrah, 61004, Basrah, Iraq
drammarakesh@gmail.com

Abstract

The effect of impeller flow type and rotation speed on the fluid in mixing tank design under standard configurations investigated to analyses the fluid velocity, turbulent intensity and path lines. In this theoretical study, the fluid motion inside the mixing tank was investigated by solving Navier-Stokes equation and standard k-ε turbulent model in 3-dimensions, for incompressible and turbulent flow. Two types of flow with three types of impellers were investigated, axial-flow with (Lightnin200 and generic impellers) and radial-flow with (Rushton turbine). All impellers evaluated under rotation velocity variation between 10 – 115 rpm. The results showed a direct proportional relationship between the impeller and turbine rotation speed with the fluid velocity in mixing vessel. Also, this case matches with the turbulent intensity and path lines.

Keywords- Impeller . Mixing tank. k-ε Turbulent model . Lightnin200. Generic. Rushton Turbine .

الخلاصة

إن لسرعة دوران المروحة ونوع تدفق المائع خلال المراوح المستخدمة في عمليات الخلط تأثير كبير على حركة المائع في خزانات الخلط المصممة وفقا للمعايير القياسية. في هذه الدراسة النظرية تمت دراسة وتحليل ومناقشة تأثير سرعة دوران المروحة على سرعة المائع وشدة الاضطراب ومسارات جريان المائع . تم استخدام معادلة Navier-Stoke والأنموذج k-ε الخاص بالجريان الاضطرابي لدراسة حركة المائع في خزان الخلط الثلاثي الإبعاد مع مراعاة استخدام نموذج معالجة الدالة قرب الجدار الخاص بخزان الخلط وذلك من خلال الحقيبة البرمجية المسماة MixSim الخاصة بتصميم ودراسة الموائع في عمليات الخلط المختلفة والتي هي جزء من الحقيبة البرمجية الشاملة FLUENT 6.2.

تمت دراسة نوعين من تدفق الموائع خلال مراوح الخلط هما الجريان المحوري متمثلا بـــنوعين من الـــمراوح الأول هو , *Lightnin200* والثاني هو *Generic* . أما النوع الثاني من التدفق هو التدفق النصف قطري متمثلا بـــ *Rushton turbine* . تم اختبار جميع أنواع المراوح بسرعة دورانيه تتراوح من 10 إلى 115 دورة في الدقيقة . أظهرت النتائج إن هناك علاقة طردية بين كل من سرعة المائع وشدة اضطرابه مع السرعة الدورانيه للمراوح وكذلك الحال مع مسارات حركة المائع .

كلمات مفتاحية :– مروحة. حوض الخلط . نموذج *k-ε* الاضطرابي . توربينة روشتون

1. Introduction

1.1 The Fundamentals of Mixing

The word mixing describes the specific blending, mingling, or commingling of coagulating chemicals or materials with water in order to create a more or less homogeneous single – or multiple – phase system.

The word stirring describes the disturbing of the flow pattern of a fluid in mechanically orderly way for the purpose of effecting a dynamic redistribution of particles by the induced turbulence.

Random rather than orderly turbulence can be distinguished by term agitation.

Mixing is a brief operation seeking a quick response, often in advance of stirring or agitation, whereas stirring and agitation are more protracted operations normally aiming at the conjunction of suspended particles or flocs (Gordin *et.al.*, 1985).

Mixing patterns are often complex and difficult to describe , so usually classify mixers based upon how closely they approximate one of two idealized flow patterns , plug flow or complete mixing (Louise , 1993) .

1.2 Ideal Plug Flow

This type of mixing can explain as that, each volume of water remains in the reactor for exactly the same amount of time. If a slug of dye were injected into the flow as a tracer, then all the dye would appear at the outlet at the same time. Ideal plug flow is very difficult to achieve. In general, the reaction basin must be very long in comparison to its width or diameter before the mixing pattern begins to approximate plug flow (Louise , 1993).

1.3 Complete Mixing

Basins are always instantaneously blended throughout their entire volume. As a result, an incoming volume of water immediately loses its identity and is intermixed with the water that entered previously. A complete-mix reactor is also called a back-mix reactor because its contents are always blended backwards with the incoming flow. If a slug of dye tracer was injected into the basin, then some of it would immediately appear in the outgoing flow. The concentration of dye would drop steadily as the dye in the basin back mixed with the clear incoming water and was diluted by it (Nicholas , 2002).

2. Mixing Intensity

The type and intensity of agitation are also important. Turbulent mixing, character-ized by high velocity gradients G, is desirable in order to provide sufficient energy for inter-particle collisions. In order to provide the required energy propeller and turbine mixers are used. Turbine mixers are more suited than propeller. Propellers put more energy into circulating the basin contents, while turbine mixers shear the water, inducing the higher velocity gradients and the multi directional velocity currents that promote particle collisions (McGraw, 1973).

In a turbine-type complete-mix basin , the mixing intensity will not be uniform throughout the basin , but the impeller discharge zone occupies about 10 percent of the total volume and has a shear intensity approximately 2.5 times the average (McGraw., 1973).

There is an upper limit to mixing intensity because high shear conditions can break up micro-flocs and delay or prevent visible floc formation(Louise , 1993).

(Casy, 1997) found in experimental work that the geometry and speed for several type of impellers are vary within rang 0.2 – 0.6 m/s with the relative blade velocity in the tank is about 0.75 time the peripheral velocity and the drag coefficient Cd for flat blades is about 1.8, also, the paddle blade area is usually between 15 % to 25 % of tank cross section area, and the detention time about 20 – 40 minute for optimum flocculation process. (Holland and Chapman, 1966) use different types of impeller and its path lines generated, reported that the axial – flow generates a constant pumping action toward the bottom of mixing tank at first stage and then followed by circulation to the top of the mixing tank at the second stage after that the rapid return to the impeller zone at the final stage. On the other hand , the radial-flow impeller direct the fluid flow in the radial direction out ward from the impeller which mostly circulates in the region above the impeller , before slowly returning to the impeller zone . **(**Alves and Barata , **1997)** studied the mixing process for tall tank agitated by multi-Rushton turbines to get the best dimensions for the model . The models in this study were structured by using computation fluid dynamics (CFD) with flat bottom cylindrical vessel of inner diameter DT = 0.292m equipped with four baffles of width =DT / 10 . Stirring was provided by Rushton turbine agitator of diameter =DT/3 driven by a variable speed 0.75 KW. AC.

motor. The off-bottom clearance of the lowest turbine was DT/2. The working liquid were tap water and glycerol solution and liquid depth were set to 3DT. The spacing between turbines was DT to prevent hydrodynamic interaction between them under those condition the mixing process becomes more convenient by using multi impellers and gets a stabile homogenous for lees mixing tank . **(**Wei-Ming and Ming-Ying , **1997)**studied the effect of baffle design on the liquid mixing in stirred tank with standard Rushton turbine impellers , they noted that the insertion of the appropriate number of baffles clearly improves the extent of liquid mixing . The width and the number of the baffles affect the extent of liquid mixing of the single impeller system for N=3.33 rps in term of mixing time. The mixing time decreases steeply with the increase of the width of baffles first, and then it soon reaches a constant value as B/DT exceeds 0.1 where B is baffle width and DT is tank diameter. It is interesting to note that this leveling of values tend to decrease as the number of baffles increases in the range n_b <8 and B/DT > 0.2 . The model of this study was done by using Fluent software and the k-ε turbulent model was adopted to determine the Reynolds stresses. Also they determined the optimum number of baffle.

3. Physical Model

Since the flow in mixing tank are complex and change from zone to zone, (i.e. from high turbulent level at impeller zone to less turbulent flow near the wall of tank) so, it is necessary to use mathematical models to predict such flow fields .

3.1 The Standard Configuration of Designing Mixing Tank

The design of mixing tank depending on the following standard configuration provides an arbitrary criterion for sufficient mixing in stirred tanks (Selomulya, 2001) , (Georgy, 1991) .

1. The impeller diameter , (***D***) **= 1/3** of the tank diameter , (***DT***) .
2. The impeller height from the bottom of the tank (impeller clearance) , (***Hi***) = impeller diameter , (***D***) .
3. The impeller blade width , (***q***) = (***1 / 5***) impeller diameter , (***D***) .
4. The impeller blade length , (r_i) = (***1 / 4***) impeller diameter , (***D***) .
5. Length of impeller blade mounted on the central disk (s_i) = (**1 / 8**) impeller diameter , (***D***) .
6. Liquid height , (***Hl***) = tank diameter , (***DT***) .

3.2 The Model of Present Study

The mixing tank design depends on the above standard configuration in 3-D. The model consists of the following items (figure 1) :

1- Cylindrical tank with 25 *cm* diameter and 32 *cm* height with flat bottom style .
2- Inlet tube with 0.8 *cm* inner diameter .
3- Out let tube with 0.8 *cm* inner diameter .
4- Top shaft with 0.6 *cm* diameter .

Using three types of impellers with two types of flow: axial-flow (Lightnin , 200) and generic impeller (high efficiency) and radial-flow (Rushton turbine) . The specification of the three type of impeller show in table (1) .

Table (1) Specification of Impellers Used in the Mixing Tank Model

specification	Impeller type		
	Lightnin 200	Rushton turbine	Generic
No. of blades	3	6	3
Blade width at root (m)	0.016	0.016	0.016
Blade width at tip (m)	0.016	0.016	0.016
Blade thicknesses (m)	0.001	0.0016	0.002
Hub cord angel (deg.)	45 ^{o}	90 ^{o}	45 ^{o}
Tip cord angel (deg.)	45 ^{o}	90 ^{o}	20 ^{o}
Hub diameter (m)	0.0155	0.02081	0.018
Hub height (m)	0.0135	0.01665	0.02
Inner diameter (m)	-	0.042	-
Disk diameter (m)	-	0.0624	-

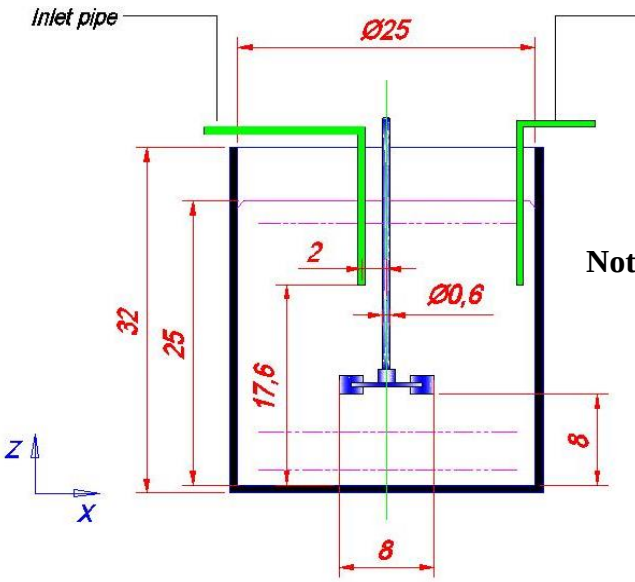

Note: all dimension in cm.

Figure (1) Geometry with all Dimensions.

3.3 Assumptions

The following assumptions are used to simplify the proposed model solution :

1- The fluid is water .
2- The fluid has constant properties .
3- Steady state conditions .
4- The detention time of fluid is 1800 sec , that means the study of fluid motion and path lines in this period .
5- The model case is turbulence , and stander ***k-ε*** model is used.
6- No slip at wall .
7- The impeller has constant rotation velocity .

3.4 Boundary Conditions

Referring to figure (1) which illustrates the boundary condition in the mixing tank where the boundary conditions of this model can be summarized as follows :

1- On the tank wall , the velocity is taken to be zero (no slip) .
i . e . *U=0 , V=0 and W* = 0 in the Z , R and θ direction .

2- At the symmetric line , $\frac{\partial \phi}{\partial n} = 0$ (Anderson., 1980; Versteeg and Malasekera, 1995) .

i.e. $\frac{\partial U}{\partial r} = \frac{\partial V}{\partial r} = \frac{\partial W}{\partial r} = 0$

3- The impeller velocity = $\omega \times r_i$

4- The initial values for ***k*** and ***ε*** are

$$k = \frac{3}{2}(U_{ref} T_i)^2 \quad , \qquad \varepsilon = C_\mu^{3/4} \frac{k^{\frac{3}{2}}}{l} \quad , \qquad l = 0.07^2 \frac{D}{2}$$ (Anderson , 1980) .

3.5 The k-ε Turbulence Model

The standard (***k-ε***) model is a semi empirical model based on model transport equation for two turbulent properties , kinetic energy (***k***) and its dissipation rate (***ε***) .

For turbulence kinetic energy (*k*)

$$\rho\bar{u}\frac{\partial k}{\partial z} + \rho\bar{v}\frac{\partial k}{\partial r} + \rho\bar{w}\frac{\partial k}{\partial \theta} = \frac{\partial}{\partial z}\left(\frac{\mu_t}{\sigma_{k,t}}\frac{\partial k}{\partial z}\right) + \frac{1}{r}\frac{\partial}{\partial r}\left(\frac{\mu_t}{\sigma_{k,t}} r \frac{\partial k}{\partial r}\right) + \frac{1}{r}\frac{\partial}{\partial \theta}\left(\frac{\mu_t}{\sigma_{k,t}}\frac{\partial k}{\partial \theta}\right) \quad (3-1)$$

$$-\rho\varepsilon + \mu_t G$$

For energy dissipation rate (*ε*)

$$\rho\bar{u}\frac{\partial \varepsilon}{\partial z} + \rho\bar{v}\frac{\partial \varepsilon}{\partial r} + \rho\bar{w}\frac{\partial \varepsilon}{\partial \theta} = \frac{\partial}{\partial z}\left(\frac{\mu_t}{\sigma_{\varepsilon,t}}\frac{\partial \varepsilon}{\partial z}\right) + \frac{1}{r}\frac{\partial}{\partial r}\left(\frac{\mu_t}{\sigma_{\varepsilon,t}} r \frac{\partial \varepsilon}{\partial r}\right) + \frac{1}{r}\frac{\partial}{\partial r}\left(\frac{\mu_t}{\sigma_{\varepsilon,t}}\frac{\partial \varepsilon}{\partial \theta}\right) \quad (3-2)$$

$$+ C_1 \frac{\varepsilon}{k}\mu_t G - C_2 \frac{\varepsilon^2}{k}$$

Where *G* is referred to the generation term and is given by (Versteeg and Malasekera, 1995) :

$$G = 2\left[\left(\frac{\partial \bar{u}}{\partial z}\right)^2 + \left(\frac{\partial \bar{v}}{\partial r}\right)^2 + \left(\frac{\bar{v}}{r}\right)^2\right] + \left[\left(\frac{\partial \bar{u}}{\partial r}\right) + \left(\frac{\partial \bar{v}}{\partial z}\right)\right]^2 + \left(\frac{\partial \bar{w}}{\partial z}\right)^2 + \left(\frac{\partial \bar{w}}{\partial r} - \frac{\bar{w}}{r}\right)^2 \text{ ..... } (3-3)$$

The turbulent kinetic energy (***k***) and the dissipation rate of the turbulent energy (***ε***) are chosen as the two properties in order to determine the turbulent viscosity μ_t .

$$\mu_t = \frac{C_\mu \rho k^{\frac{1}{2}}}{l^{-1}} \qquad \text{..... } (3-4)$$

Where: C_μ is a constant , it is assumed that at a high Reynolds number , (***ε***) value to be proportional to $k^{\frac{3}{2}} / l$, the above equation becomes :-

$$\mu_t = \frac{C_\mu \rho k^2}{\varepsilon} \qquad \text{..... } (3-5)$$

The value of the constants in the (***k-ε***) model shows in table (2) below .

Table (2) value of (k-ε) constant (Versteeg and Malasekera, 1995 ; Marco and Francesco, 1990)

C_1	C_2	C_μ	$\sigma_{k,t}$	$\sigma_{\varepsilon,t}$
1.44	*1.92*	*0.09*	*1*	*1.3*

3.6 Governing Equations

The description of the fluid motion in the mixing tank is made by solving the average differential equation of mass (continuity) and momentum equation model equation by considering the infinite control volume with cylindrical coordinate .

3.6.1 Continuity Equation

The net flow of mass across the boundary of a control volume is zero in steady state flow. The continuity equation can be written as conservation of mass equation with the following form

$$-\frac{\partial}{\partial z}(\bar{u})+\frac{1}{r}\frac{\partial}{\partial r}(r\bar{v})+\frac{1}{r}\frac{\partial}{\partial \theta}(\bar{w})=0 \qquad \text{..... (3 – 8)}$$

3.6.2 Momentum Equation

The general momentum equations governing the fluid motion for three dimensions in cylindrical coordinate are (Ronald , 1984) :

In z – direction :

$$\rho\left[\bar{u}\frac{\partial}{\partial z}(\bar{u})+\bar{u}\frac{1}{r}\frac{\partial}{\partial r}(r\bar{v})+\bar{u}\frac{1}{r}\frac{\partial}{\partial \theta}(\bar{w})\right]=-\frac{\partial \bar{p}}{\partial z}+2\frac{\partial}{\partial z}\left(\mu_{eff}\frac{\partial \bar{u}}{\partial z}\right)+\frac{1}{r}\frac{\partial}{\partial r}\left[r\mu_{eff}\left(\frac{\partial \bar{u}}{\partial r}+\frac{\partial \bar{v}}{\partial z}\right)\right]$$

$$+\frac{1}{r}\frac{\partial}{\partial \theta}\left[\mu_{eff}\left(\frac{1}{r}\frac{\partial \bar{u}}{\partial \theta}+\frac{\partial \bar{w}}{\partial z}\right)\right] \qquad \text{..... (3 –31a)}$$

In r – direction :

$$\rho\left[\bar{v}\frac{\partial}{\partial z}(\bar{u})+\bar{v}\frac{1}{r}\frac{\partial}{\partial r}(r\bar{v})+\bar{v}\frac{1}{r}\frac{\partial}{\partial \theta}(\bar{w})\right]=-\frac{\partial \bar{p}}{\partial r}+\frac{\partial}{\partial r}\left[\mu_{eff}\left(\frac{\partial \bar{v}}{\partial z}+\frac{\partial \bar{u}}{\partial r}\right)\right]+\frac{2}{r}\frac{\partial}{\partial r}\left[r\mu_{eff}\left(\frac{\partial \bar{v}}{\partial r}\right)\right]$$

$$+\frac{1}{r}\frac{\partial}{\partial \theta}\left[\mu_{eff}\left(\frac{1}{r}\frac{\partial \bar{v}}{\partial \theta}+r\frac{\partial\left(\frac{\bar{w}}{r}\right)}{\partial r}\right)\right]+\rho\frac{\bar{w}^2}{r}-\frac{2\mu_{eff}}{r}\left(\frac{1}{r}\frac{\partial \bar{w}}{\partial \theta}+\frac{\bar{v}}{r}\right) \qquad \text{..... (3 – 32a)}$$

In Θ - direction :

$$\rho\left[\bar{w}\frac{\partial}{\partial z}(\bar{u})+\bar{w}\frac{1}{r}\frac{\partial}{\partial r}(r\bar{v})+\bar{w}\frac{1}{r}\frac{\partial}{\partial \theta}(\bar{w})\right]=-\frac{1}{r}\frac{\partial \bar{p}}{\partial \theta}+\frac{\partial}{\partial z}\left[\mu_{eff}\left(\frac{\partial \bar{w}}{\partial z}+\frac{1}{r}\frac{\partial \bar{u}}{\partial \theta}\right)\right]+$$

$$\frac{1}{r}\frac{\partial}{\partial r}\left[\mu_{eff}\left(r\frac{\partial \bar{w}}{\partial r}+\frac{\partial \bar{v}}{\partial \theta}-\bar{w}\right)\right]+\left[\frac{\mu_{eff}}{r}\left(r\frac{\partial\left(\frac{\bar{w}}{r}\right)}{\partial r}+\frac{1}{r}\frac{\partial \bar{v}}{\partial \theta}\right)\right]-\frac{\rho\bar{w}\bar{v}}{r}+\frac{2}{r}\frac{\partial}{\partial \theta}\left[\mu_{eff}\left(\frac{1}{r}\frac{\partial \bar{w}}{\partial \theta}+\frac{\bar{v}}{r}\right)\right] \qquad \text{.....(3 – 33a)}$$

4. Simulation Setting

To setup the simulation program in FLUENT , the following were carried out :

1- The meshed geometry of simulation case study were imported from Gambit into FLUENT .

2- Turbulent flow model was selected (solver) .

3- The fluid was defined and it's variables selected .
4- The k-ε model was chosen as the turbulent model .
5- Specify the operation conditions .
6- Defining the boundary condition concerned .
7- The starting values of velocities , pressure and turbulent parameters
8- Appropriate residual conditions were defined .

4.1 The meshes

The boundary of the shapes was mashed by boundary layer and the rest of the geometry was auto meshed with schema called tetrahedral and triangular types as shown in figure (2)

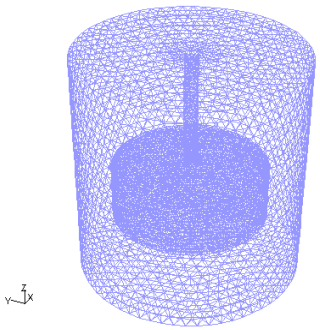

A

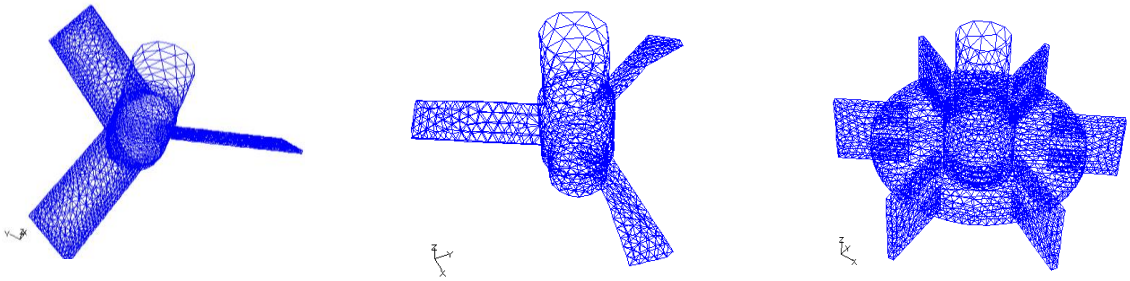

Lightnin200 **Generic** **Rushton turbine**

B

Figure (2) (A) Shows the Mesh of Geometry and (B) Shows the Mesh of present study Impellers

5. Results and Discussion

The value of velocity magnitude can be evaluated relative to impeller radius. When the impeller radius is equal to zero so the value of impeller speed would be equal to zero too, while the maximum velocity can be achieved at the tip of impeller blade. This behavior could be repeated for three types of impeller. However figure (3) shows the velocity distribution along of the blade of impeller when the impeller blade have radius between zero to 0.04m .

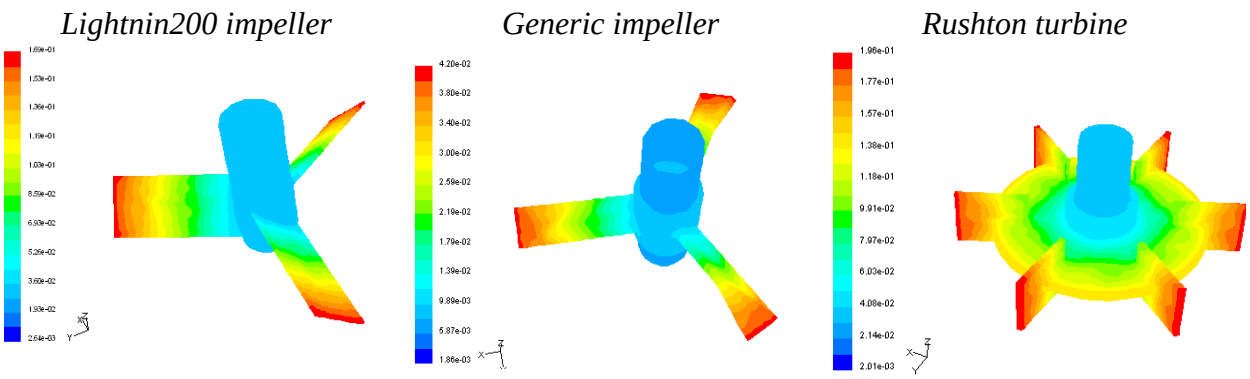

Figure (3): The velocity distribution along of the blade of impeller

Figure (4) shows the velocity vectors and contours for impellers at 10 rpm . For Lightnin200 impeller, the figure shows that the fluid motion is started from impeller zone to the bottom of mixing tank at first stage then change direction to the upper region of tank in second stage , in the third stage, the flow retunes to the impeller zone with high velocity .

This behavior is referred to that the fluid flow is proportional with impeller pumping direction .

Anyway , the fluid upper and lower region of impeller is mainly affected with circulation motion of fluid , while the fluid near the top zone of mixing tank is less effected with fluid motion . Also, it can note that the fluid near the tip of the impeller blade is not affected with impeller rotation where this clearly appears in the contour of velocity in figure (4) , this behavior due to the previous zone is far from the pumping direction of impeller .

In the same figure, for the Generic impeller, the velocity vectors of fluid motion is approximately similar to the fluid motion of Lightnin200, but the major difference is occur in the fluid profile near the tip of impeller blade shows a largely influence with impeller rotation but it's not affected with impeller pumping direction motion. Therefore, the small eddies are generated in this region due to the impeller blade design as shown in figure (4) .

However, the flow behavior is different with the Rushton turbine . Figure (4) illustrates the pumping direction is started from the tip of turbine blade then the fluid divided into two parts . The first one in the upper region from the turbine and circulated from the tip turbine bled to the upper direction of the mixing tank then return to the turbine zone where most of fluid in this zone is influenced with this circulation motion. The second part take the same behavior of the first part but in the lower region of the turbine .

The fluid velocity generated as a result of impeller motion is varies with each type of impeller. The higher velocity value occur with Ruston turbine is 3.27×10^{-2} m/s , while lower magnitude occur with generic impeller 1.81×10^{-2} m/s

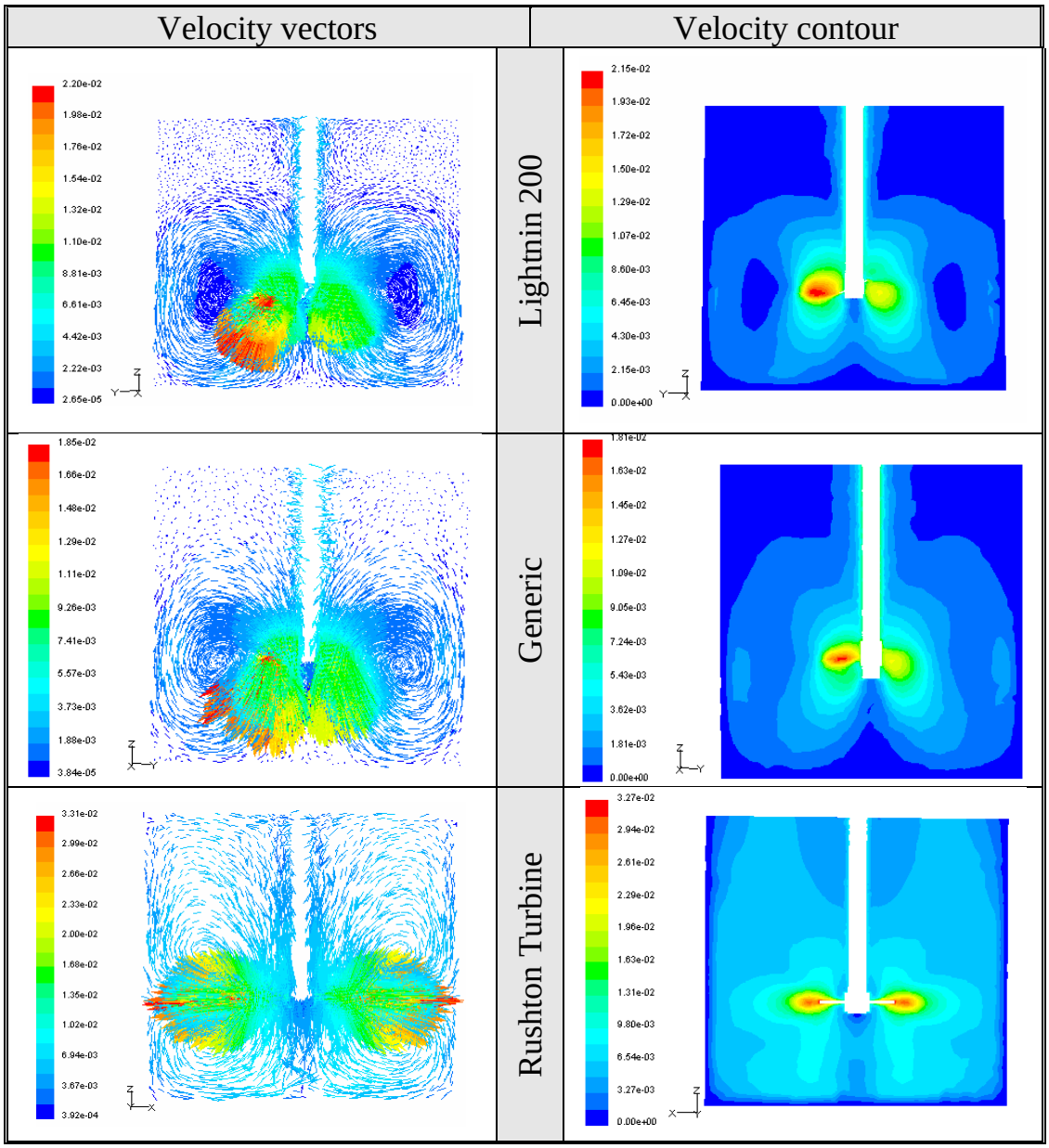

Figure (4) :The velocity vectors and contours for impellers at 10 rpm

Figure (5) shows the value of fluid velocity for each type of impellers at 10 rpm , as a function of tank radius and taking into account the line of symmetry .

For lightnin200 impeller the fluid velocity at zone of mixing tank between radius 0.005-0.03 m is about 0.0015 m/s and then increases with the increment of tank radius until it reaches the maximum value which is about 0.0042 m/s . At mixing tank zone between the tank radius 0.03-0.085 m the fluid velocity decreases from 0.0042 m/s to about 0.0009 m/s with the increment of tank radius. The last stage at zone between tank radius 0.085-0.11m the fluid velocity take a direct proportional relation with the increment of tank radius, the fluid velocity increases from 0.0008 m/s to 0.0011m/s , then decreases to 0.009 m/s near the wall .

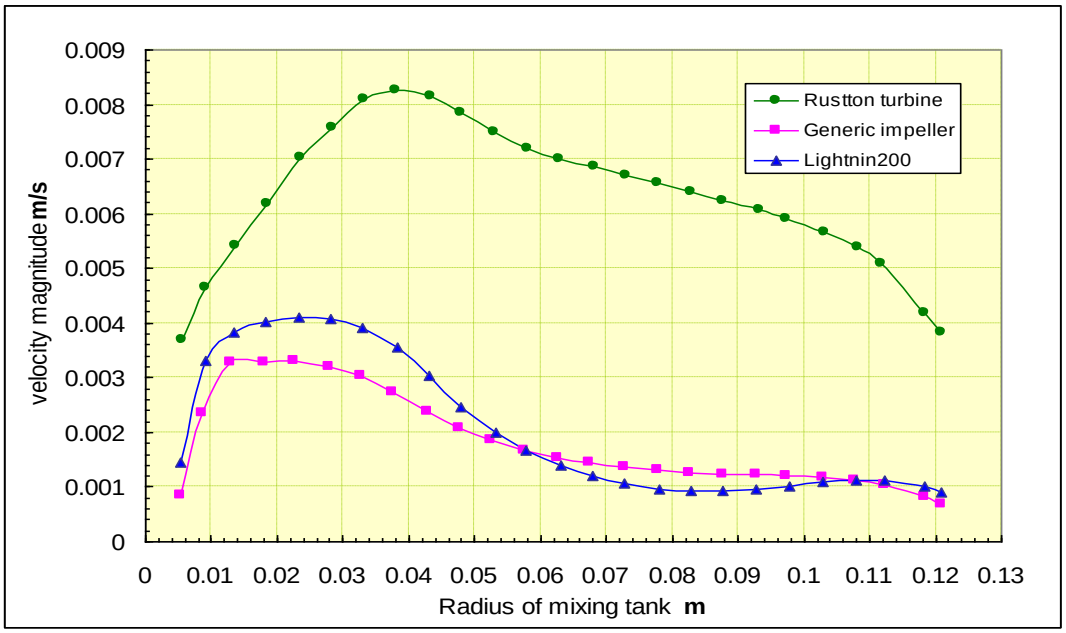

Figure (5) : The value of fluid velocity for each type of impellers at 10 rpm

From above illustrates it can explain the maximum fluid velocity occurs at impeller zone in the mixing tank , and for zone far from impeller the fluid velocity decreases since the fluid becomes less effects with the impeller motion because if far from impeller zone . At the last zone the effect of impeller pumping capacity and direction clearly appear, it's increase the fluid velocity in this zone , then the velocity decreases at near the wall because the velocity at wall is zero and increases gradually to word the impeller zone.

The fluid velocity with generic impeller at 10 rpm takes similar behavior to Lightnin200 impeller. The fluid velocity at zone of mixing tank between radius 0.005-0.03 m is about 0.0008 m/s and then increases with the increment of tank radius until it reaches the maximum value which is about 0.0033 m/s . At mixing tank zone between the tank radius 0.024-0. 12 m the fluid velocity decreases from 0.0033 m/s to about 0.007 m/s with the increment of tank radius .

For Rushton turbine the magnitude of fluid velocity is higher than the Lightnine200 and generic impeller but, the fluid velocity behavior is similar to the axial flow impeller, the highest value at impeller zone and decreases at other zone in mixing tank. Velocity increasing at impeller zone and decreasing with increment of mixing tank radius.

5.1 Effect of Impeller Rotation Speed on the Turbulent Intensity

Figures (6 and 7) show the contour of turbulent intensity at 10 rpm. For Lightnin200 impeller at 10 rpm, in the beginning the turbulent intensity is generated at the zone of impeller (highest velocity) , after this step the turbulent intensity expands in all direction with reduction of turbulent values . The turbulent intensity in the lower zone of the impeller is greater than the upper zone because the area of lower zone is smaller than the upper zone with taking into account the constant pumping capacity of impeller at the same rotation speed .

The same behavior is occurred with the generic impeller type at same rotation speed but with less magnitude in turbulent intensity value, because the velocity generated with this type is less than the Lightnin200 type .

Rushton turbine at 10 rpm gives other indication , it is clearly to note the turbulent intensity generated with the same start point of Lightnin200 and Generic impeller but the shape of expansion is approximately to be circled and continues into propagate to the all mixing tank zones .

The profile for turbulent intensity shows the highest level with Rushton turbine and the lowest level with generic impeller but, for Lightin200 impeller, the turbulent intensity is less relative to Rushton turbine and great relative to the generic impeller with small difference.

The turbulent intensity is increased for axial-flow impellers and also for radial-flow turbine with increment of the rotation speed.

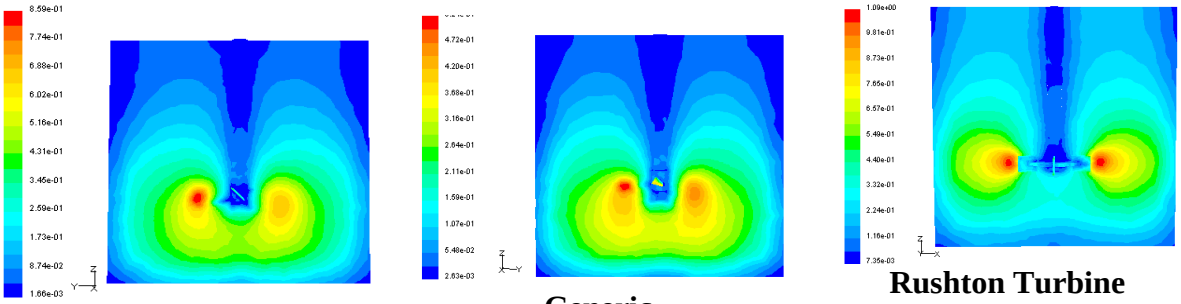

Figure (6) : The contour of turbulent intensity at 10 rpm

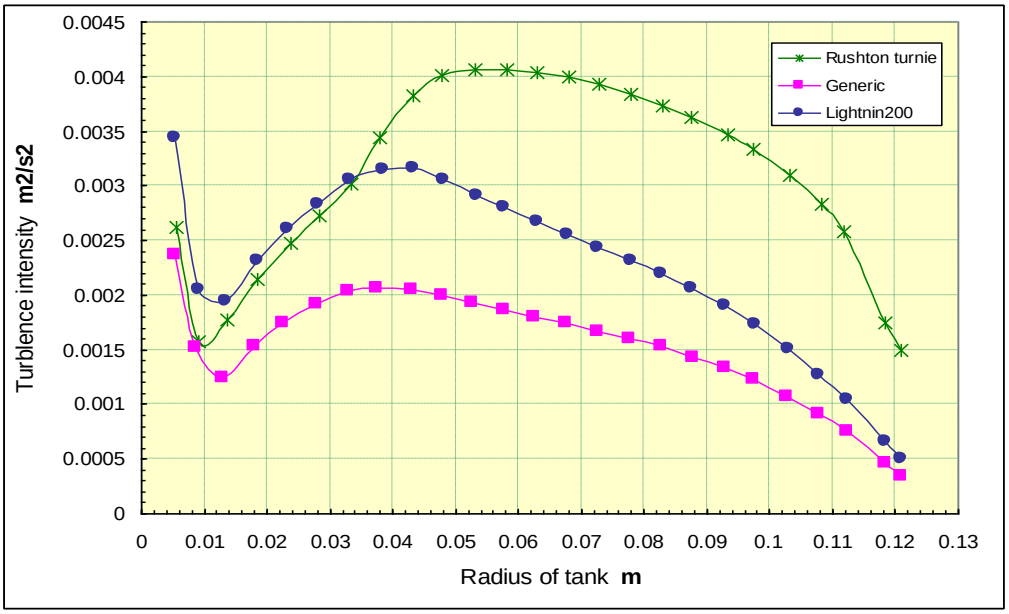

Figure (7) The contour of turbulent intensity with tank radius at 10 rpm

5.2 Effect of Impeller Rotation Speed on the Path Lines

Figure (8) shows the path lines for the axial-flow impeller and radial-flow turbine for impeller rotation speed varies between 10 rpm .

The drawing for path lines are always in 3-D, and it is difficult to get clear image to explain the path lines of fluid motion especially in mixing tank. But it is important to study the shape of path line and its effect on floc formation .

The path lines for Lightnin200 at 10 rpm indicate that the impeller generate a constant pumping action toward the bottom of vessel followed by the circulation to the top of the vessel and return to impeller zone. The fluid in the vessel is not fully influence with the patterns of circulation, where the top part is less effective, because this zone is far from impeller zone.

The shape of path lines have taken approximately uniform shapes with one plane (i.e. for one path line is stared from impeller zone to the bottom of vessel then circulated to the top of vessel with straight line and return to impeller zone again where all this occur without any deflection with the path) . That is mean the tangential velocity very small so it's effect not appear .

The Generic impeller adopts the same behavior with Lightnin200 impeller , but the tangential velocity is more affected on the path of fluid motion . This is due to the tip design of impeller blades. This case is different with radial-flow turbine at the same rotation speed with axial-flow impellers .

The Rushton turbine is directed the fluid flow in the radial direction outward from the impeller, which is mostly circulation in the region above the impeller and slowly returned to the impeller zone .

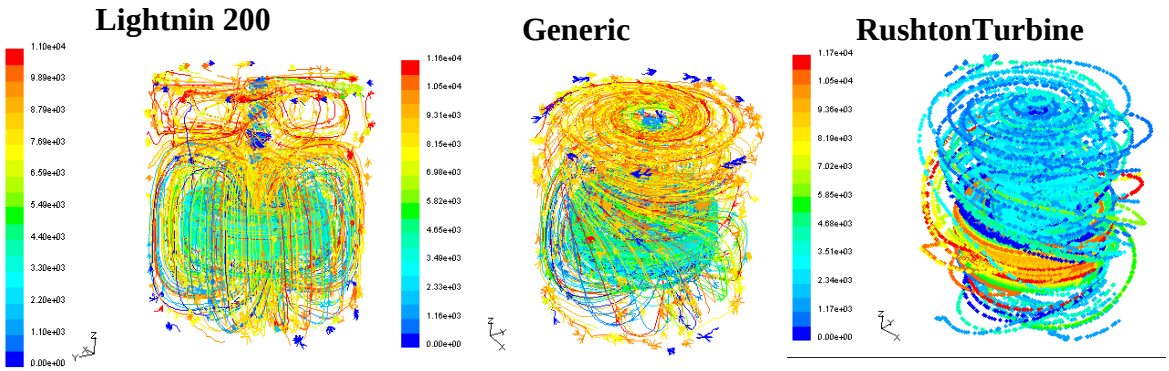

Figure (8) : The path lines for the axial-flow impeller and radial-flow turbine for impeller rotation speed varies between 10 rpm .

6. Conclusions

From the results, it is concluded that :

1- The program MixSim is appropriate to modeling and solving problems of fluid motion and velocity in mixing tank.

2- For the same type of impeller flow (axial-flow), there are different results. The Lightin200 impeller is more suitable than Generic in flocculation process.

3- For the different type of impeller flow, axial-flow and radial-flow, the results shows that, the radial-flow turbine is more appropriate than axial-flow impellers for flocculation process.
4- When increase the impeller rotation speed, the fluid motion and the turbulent intensity increases.

7. References

A hand book , 1973 ," Water Quality and Treatment " third edition. Inc. McGraw-Hill Book Company prepared by the American Water Works Association. PP: 73.

Alves S. S. , Vasconcelos J. M. T. and Barata J. , Part A march 1997," Alternative Compartment Models of Mixing in Tall Tank Agitated By Multi-Rushton Turbine " Institution of chemical engineers Trans IchmE , vol. 75. PP: 334 – 335.

Anderson , J. , 1980, " Computational Fluid Dynamic " . McGraw – Hill .

Georgy T. , Franklin , L. Burton , 1991 ," Wastewater Engineering , Treatment , Disposal , And Result " . McGraw-Hill series in water resources and environmental engineering, 3rd edi. PP: 217.

Gordin M. Fair, John C. Geyer, Danial A. Okun, 1985, " Water Purification and Wastewater Treatment and Disposal ". John Wily & Sons, New York.

Holland F.A. and Chapman F.S. , 1966, " Liquid Mixing and Processing in Stirred Tank ". Reinhold publishing corporation, New York.

http: // www. Zeta–meter.com .

Louise R. , 1993 ," Every Thing You Want Know About Coagulation and Flocculation " . Zeta-meter , Inc. fourth edition., April.

Marco Casonto and Francesco Gallerano , 1990 ," A finite Difference Self –Adaptive Mesh Solution Of Flow In A Sedimentation Tank " . International journal for numerical method , vol. 10 , John Wily and Sons. PP: 697-711.

Nicholas P. Cheremisinoff , 2002," Hand Book of Water and Wastewater Treatment Technologies " . Butterworth -Heinemann.

Ronald l. panton , 1984 ," Incompressible Flow " . A Wiley–interscience publication , John Wily and Sons , 2nd edi.

Selomulya,G. , 2001, " The Effect of Shear on Flocculation and Floc Size ". PhD. Thesis, university of new south Wales.

T-J. Casy , 1997, " Unite Treatment Processes in Water and Wastewater Engineering " .Wiley.

Versteeg H.K. and W.Malasekera, 1995, "An Introduction to Computational Fluid Dynamics , The Finite Volume Method " . Longman scientific and technology.

Wei-Ming Lu , hong – Zhang Wu and Ming-Ying Ju . , 1997, " Effect of Baffle Design on The Liquid Mixing in An Aerated Stirred Tank With Standard Rushton Turbine". Chemical engineering science, vol. 52, Nos. 21:22. PP: 3843-3851.

Nomenclature

English Symbols

Symbols	Description	SI Unit
D	Impeller diameter	m
DT	Diameter of mixing tank	m
d_{floc}	Floc diameter	µm
F	Force	N

G	Velocity gradient in sheared fluid	S^{-1}
k	Constant	
l	Mixing length	
M	Mass	kg
N	Impeller rotation speed	rev/min
p	Pressure	N / m^2
r	Radius of mixing tank	m
S_ε	Source term in k-ε model	

Greek symbols

Symbols	Description	SI Unit
α	Relaxation factor	
ρ	Density	kg / m^3
ε	Dissipation rate of kinetic turbulence energy	m^2 / s^3
k	Turbulent kinetic energy	m^2 / s^2
μ	Dynamic viscosity	Pa.s
μ_t	Turbulent viscosity	Pa.s
μ_e	Effective viscosity	Pa.s
υ	Kinematics viscosity	m^2/s^2
σ_k	Turbulent Prandtl constant in k- equation	
σ_ε	Turbulent Prandtl constant in ε- equation	
τ	Shear stress	N / m^2

Group Abbreviations :

Symbols	Description
CFD	Computational Fluid Dynamics
CLSM	Confocal leaser scanning microscopy
GAMBIT	Package software

Prefix :

Symbols	Description
∂	Partial gradient
∇	Gradient operator

Dimensionless Group :

Symbols	Description
GT	Camp's number
Re	Reynolds number